Collective structures and band termination in ^{107}Sb

D. R. LaFosse, C. J. Chiara, D. B. Fossan, G. J. Lane,* J. M. Sears, J. F. Smith,† and K. Starosta‡
Department of Physics and Astronomy, State University of New York at Stony Brook, Stony Brook, New York 11794-3800

A. J. Boston, E. S. Paul, and A. T. Semple
Oliver Lodge Laboratory, University of Liverpool, P.O. Box 147, Liverpool L69 7ZE, United Kingdom

M. Devlin§ and D. G. Sarantites
Department of Chemistry, Washington University, St. Louis, Missouri 63130

I. Y. Lee and A. O. Macchiavelli
Nuclear Science Division, Lawrence Berkeley National Laboratory, Berkeley, California 94720

A. V. Afanasjev‖ and I. Ragnarsson
Department of Mathematical Physics, Lund Institute of Technology, Box 118, S-22100 Lund, Sweden
(Received 21 January 2000; published 7 June 2000)

High-spin states in the near proton-dripline nucleus ^{107}Sb have been identified, and collectivity in this nucleus has been observed for the first time in the form of two rotational bands. One of the observed rotational structures is a $\Delta I=1$ band, and is interpreted as based on a $\pi(g_{9/2})^{-1}\otimes\pi(g_{7/2}d_{5/2})^2$ proton configuration. A second structure has $\Delta I=2$ character, and is explained as being based on a $\pi h_{11/2}\otimes[\pi(g_{9/2})^{-2}\otimes\pi(g_{7/2}d_{5/2})^2]$ proton configuration through comparison with cranked Nilsson-Strutinsky model calculations. The calculations predict that this band terminates at a spin of 79/2 $\hbar$.

PACS number(s): 21.10.Re, 21.60.Cs, 23.20.Lv, 27.60.+j

I. INTRODUCTION

Nuclei near closed shells have long been an interesting subject of study due to the coexistence of both spherical and deformed nuclear shapes in the same nucleus. In nuclei such as the $_{50}$Sn, $_{51}$Sb, and $_{52}$Te isotopes, near-spherical single-particle and vibrational states predominate at low spins due to the small deformation of the underlying core. However, at higher spins and excitation energies, multiparticle excitations across the $Z=50$ shell gap begin to exert a significant influence. Since the energy of the $\pi g_{9/2}$ orbitals just below this shell gap increases strongly with increasing quadrupole deformation, promoting protons from these orbitals into higher-lying down-sloping orbitals has a deformation-driving effect. Configurations resulting from such excitations of one or more protons can be sufficiently deformation driving to overcome the spherical tendency of the $Z=50$ core. As a result, structures having deformation as high as $\varepsilon_2=0.3$ in the case of ^{113}Sb [1] are known in these nuclei.

The first structures of this type to be identified were $\pi(g_{9/2})^{-2}\otimes\pi(g_{7/2}d_{5/2})^2$ two-particle two-hole $(2p2h)$ decoupled rotational bands found in even-mass $^{112-118}$Sn nuclei [2], and strongly coupled structures based on $\pi(g_{9/2})^{-1}\otimes\pi(g_{7/2}d_{5/2})^2$ two-particle one-hole $(2p1h)$ high-K configurations in odd-mass $^{113-119}$Sb nuclei [3,4]. More recently, decoupled structures were found in odd-mass $^{113-119}$Sb nuclei [1,5–7]. These were interpreted as resulting from coupling of the $2p$-$2h$ excitation of the underlying $_{50}$Sn core to the valence proton occupying either a $\pi h_{11/2}$ or mixed $\pi(g_{7/2}d_{5/2})$ orbital. Interest in such structures increased dramatically with the advent of the third-generation detector arrays Gammasphere [8] and Eurogam [9]. With these devices it became possible to study more neutron-deficient Sn, Sb, and Te isotopes to very high spin; it was learned that these rotational structures gradually lose their collectivity and the nuclear shape transforms from collective near-prolate to noncollective oblate as the valence nucleons outside the ^{100}Sn core align their angular momenta with the rotation axis. Eventually all of the valence nucleons become aligned, and at this point the rotational band must terminate, having exhausted all of the angular momentum available in the configuration. This phenomenon is known as smooth band termination [10,11].

Following these structures to very neutron-deficient nuclei close to the ^{100}Sn doubly magic nucleus can further increase our understanding of these features. In particular, studying these nuclei will improve our knowledge of how deformation is generated in what are predominantly spherical nuclei. Thus, the present paper details the results of a study of the neutron-deficient nucleus ^{107}Sb, arguably the lightest $_{51}$Sb isotope that can be studied to high spin using presently available experimental techniques. High-spin states and collective

*Present address: Nuclear Science Division, Lawrence Berkeley National Laboratory, Berkeley, California 94720.

†Present address: Schuster Laboratory, University of Manchester, Brunswick Street, Manchester M13 9PL, United Kingdom.

‡On leave from: Institute of Experimental Physics, Warsaw University, Hoża 69, 00-681 Warsaw, Poland.

§Present address: LANSCE-3, Los Alamos National Laboratory, Los Alamos, New Mexico 87545.

‖Permanent Address: Laboratory of Radiation Physics, Institute of Solid State Physics, University of Latvia, LV 2169 Salaspils, Miera str. 31, Latvia.

structures have been observed for the first time in this nucleus.

II. EXPERIMENTAL DETAILS

High-spin states in ^{107}Sb were populated following the ^{58}Ni(^{58}Ni,$2\alpha p$) reaction, using a 250-MeV beam produced by the 88-Inch Cyclotron at Lawrence Berkeley National Laboratory. The isotopically enriched target consisted of two stacked self-supporting foils, each having a thickness of $\approx 500\ \mu g/cm^2$. The Gammasphere array [8] was employed to detect γ rays emitted from the residual nuclei. For this experiment Gammasphere consisted of 83 high-purity Compton-suppressed Ge detectors. The hevimet collimators ordinarily placed in front of the BGO Compton-suppression shields were removed for this experiment in order to obtain γ-ray sum-energy and multiplicity information as discussed in Ref. [12]. The Microball [13], a 4π array of 95 CsI(Tl) scintillators, was used to detect protons and α particles emitted by the compound nuclei. Finally, the front-most 15 Ge detectors were removed from Gammasphere for this experiment and replaced with NE213 liquid-scintillator neutron detectors. These play no role in the study of ^{107}Sb, however; Ref. [14] contains more information concerning the neutron detectors as employed in this experiment.

In the offline analysis, the Microball pulse-shape and timing information was used to identify protons and α particles, achieving detection efficiencies of approximately 80 and 65 %, respectively. Only those events in which two α particles and one proton were detected were chosen for the study of ^{107}Sb. The resulting data set contained approximately 6.5×10^6 events having γ-ray fold 3 or higher. Although this is a rather small number of events, the data were exceptionally clean, containing only small amounts of ^{106}Sn (from the $2\alpha 2p$ reaction channel) and ^{110}Te ($\alpha 2p$) due to the occasional nondetection of a proton or misidentification of an α particle. Finally, the $2\alpha p$-gated events were sorted into an E_γ-E_γ-E_γ coincidence cube for the construction of the level scheme. γ-ray multipolarities were assigned through directional-correlation (DCO) ratio analysis [15]. For this analysis an E_γ-E_γ matrix was created in which those detectors at back angles ($\theta \geqslant 142.6°$) were sorted against those at angles near 90° ($79.2° \leqslant \theta \leqslant 100.8°$). For all cubes and matrices, the γ-ray energies were corrected for Doppler shifts on an event-by-event basis [13]. In this approach the measured charged-particle energies and emission directions are used to obtain the velocity vector of the recoiling nucleus. The RADWARE γ-ray spectroscopy software package [16] was used extensively for all data analysis.

III. EXPERIMENTAL RESULTS

The level scheme extracted in this study is shown in the top half of Fig. 1. Pertinent information about each γ-ray transition can be found in Table I. The present study significantly extends the level scheme presented by Seweryniak *et al.* [17]. A large number of presumably near-spherical states have been added at low spins, and the level scheme has been extended to higher spins. Several modifications to the level scheme presented in Ref. [17] have also been made. In particular, only one 321-keV transition has been observed in the present study; no evidence was found for the 321-keV transition depopulating the 2856-keV level of Ref. [17]. Finally, the 1108-keV transition and the 508-1067-705-867-keV sequence have been placed above the 4100-keV level of Ref. [17].

The spin and parity (I^π) assignments shown in Fig. 1 should be considered tentative. These assignments will be discussed in the following paragraphs. Several level sequences have been labeled (a, b, c, etc.) in the top half of Fig. 1 to facilitate the discussion. A partial level scheme of ^{109}Sb taken from Refs. [18,19] is shown in the bottom of the figure; only those levels in ^{109}Sb for which the I^π assignments are firm are shown in the figure.

The DCO ratios were calibrated by measuring several known $E2$ and $E1$ transitions in ^{110}Te [20,21] and ^{112}Te [22], which were also populated in the present experiment. Stretched $E2$ transitions were found to have DCO ratios of ≈ 1.0 (as required), and stretched pure dipole ($E1$) transitions were found to have DCO ratios of ≈ 0.6, when the gating transition was of $E2$ character. However, it was found that the measured DCO ratios (including those of known pure dipole transitions) tended towards 1.0 as the spins/excitation energies of the levels involved decreased. This is consistent with an accumulated loss of nuclear spin alignment caused by hyperfine fields as the nucleus recoils into the vacuum beyond the target. As a result, the measured DCO ratios for transitions in ^{107}Sb could not be considered reliable at low spins. Table I lists those transitions for which reliable DCO ratios were extracted.

Since low-spin DCO ratios were not available, the majority of the I^π assignments given in Ref. [17] have been adopted. These assignments were made based on DCO ratio analysis and systematics. The I^π which have been adopted from Ref. [17] are the following: in sequence c, levels having $I^\pi \leqslant 17/2^+$; sequence d, $I^\pi \leqslant 19/2^+$; and sequence e, $I^\pi = 17/2^+$ and $I^\pi = 21/2^+$. The remaining I^π assignments were based on the measured DCO ratios from the present experiment, and/or a comparison to the partial level scheme shown for ^{109}Sb in Fig. 1; as can be seen in this figure, the level schemes of ^{107}Sb and ^{109}Sb are very similar, due to their underlying single-particle structure. Based on this similarity, Sequences a and b of ^{107}Sb are assigned negative parity, and spins as shown. The bottom two levels of sequence e are assigned positive parity and spins as shown. All of the DCO ratios measured in the present study are consistent with these I^π assignments. Since I^π assignments to the remaining levels cannot be made based on systematics or DCO ratios, no I^π values are shown for these levels in Fig. 1.

In addition, two mutually coincident γ-ray sequences labeled band 1 and band 2 in Fig. 1 have been identified, and assigned to ^{107}Sb based on coincidences with low-spin transitions. The energy patterns of the sequences and similarities to rotational bands known in heavier $_{51}$Sb isotopes suggest the bands have a rotational collective structure. Spectra showing these two rotational bands can be seen in Fig. 2. DCO ratios could not be measured for any of the transitions in either band. The transitions of band 1 are likely $E2$ tran-

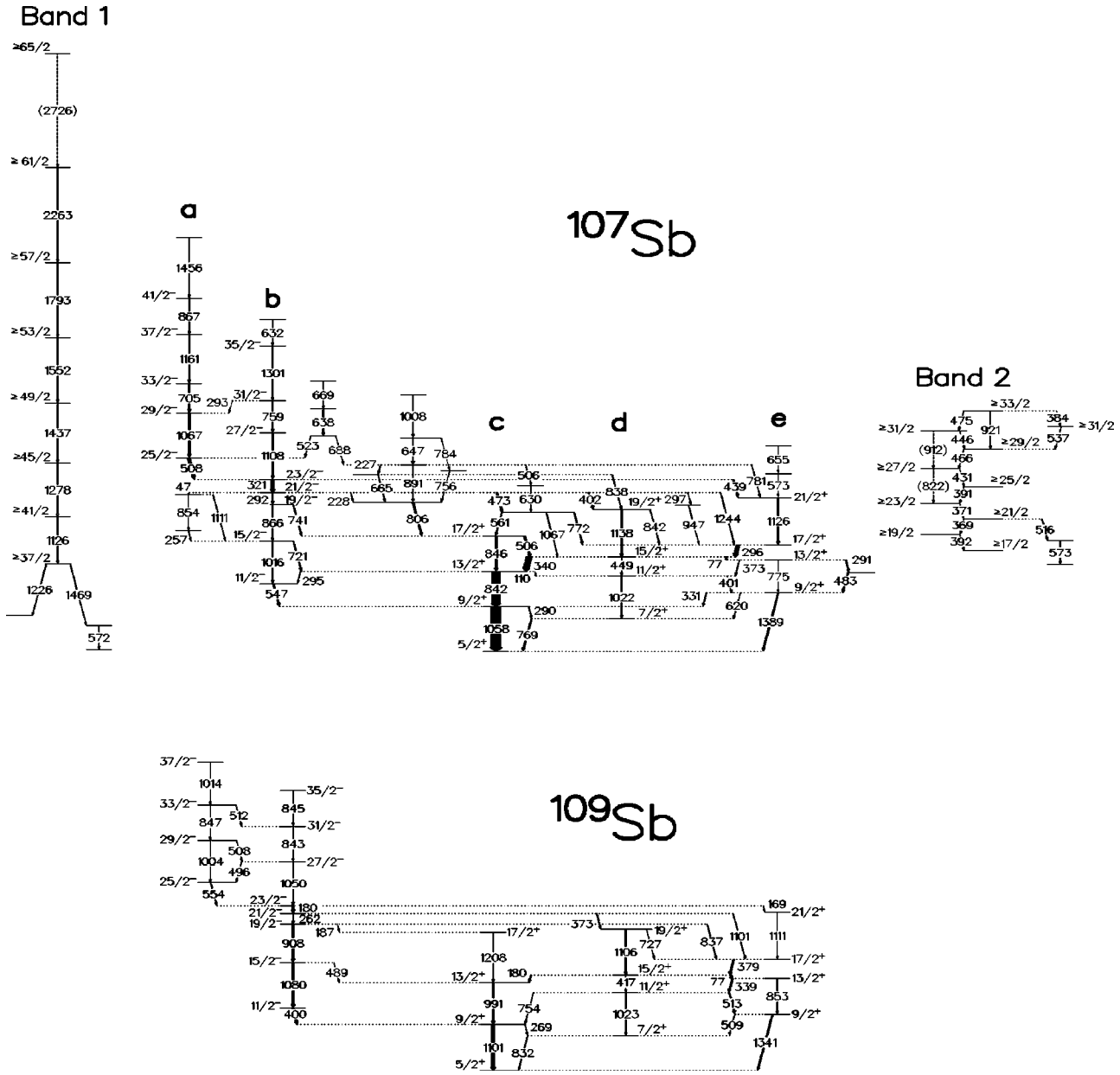

FIG. 1. Top: The level scheme of ^{107}Sb constructed in this work. Several of the low-spin level sequences have been assigned the labels a, b, c, d, or e; these are intended only to facilitate the discussion of spin assignments given in the text of the paper. Note that bands 1 and 2 are shown to the side of the main part of the level scheme since their excitation energies are unknown. Bottom: A partial level scheme of ^{109}Sb shown for comparison, taken from Refs. [18,19]. γ-ray energies are given in keV, and the widths of the arrows indicate the relative intensities of the transitions within each nucleus.

sitions, judging by their energy pattern which is characteristic of a decoupled rotational band. The ordering of the transitions has been assigned based on their relative intensities. Similarly, the more intense transitions of band 2 are assigned mixed $\Delta I=1$ character due to their energy pattern, and the presence of weak (presumably $E2$) crossover transitions at the top of the band. Also note that the ordering of some of the dipole transitions in band 2 cannot be fixed due to a lack of $E2$ crossover transitions. The fact that there are two pairs of transitions having nearly identical energies thwarts attempts to order the transitions based on intensity relationships. The population of these bands relative to the population of the ground state was found to be $\approx$2.8% (band 1) and $\approx$3.6% (band 2). Information about each of the transitions in bands 1 and 2 can be found in Table II.

The two collective bands observed in this experiment cannot be assigned spins or parities since their decay paths to states of known I^{π} could not be established. (However, several transitions responsible for removing part of the in-band intensity of bands 1 and 2 were identified, as shown in Fig. 1.) Therefore, lower limits for the spins of levels comprising these structures were established by determining the coincidence relationships between the bands and the main part of the level scheme. For example, the members of band 1 were

TABLE I. Properties of γ transitions in ^{107}Sb. The column reporting the spins of the initial and final states also shows the sequence to which the states belong, if applicable.

E_γ (keV)	I_γ (%)	DCO ratio	I_i^π	$\rightarrow$	I_f^π	Multipolarity
47(1)	[a]		$21/2^-$(b)	$\rightarrow$	(a)	
76.6(8)	[a]		$15/2^+$(d)	$\rightarrow$	$13/2^+$(e)	$M1/E2$
109.9(2)	<2.0		$13/2^+$(c)	$\rightarrow$	$11/2^+$(d)	$M1/E2$
227.1(2)	3.0(6)					
228.2(3)	<2.0		$21/2^-$(b)	$\rightarrow$		
257.4(2)	1.1(1)		(a)	$\rightarrow$	$15/2^-$(b)	
289.8(2)	5.0(3)		$9/2^+$(c)	$\rightarrow$	$7/2^+$(d)	$M1/E2$
291.4(2)	7.5(5)		$13/2^+$(e)	$\rightarrow$		
292.1(2)	4.9(4)		$21/2^-$(b)	$\rightarrow$	$19/2^-$(b)	$M1/E2$
293.3(2)	2.6(2)		$31/2^-$(b)	$\rightarrow$	$29/2^-$(a)	$M1/E2$
294.6(2)	<2.0		$13/2^+$(c)	$\rightarrow$	$11/2^-$(b)	$E1$
295.9(2)	34(2)		$17/2^+$(e)	$\rightarrow$	$15/2^+$(d)	$M1/E2$
297.1(2)	<2.0		$21/2^-$(b)	$\rightarrow$		
320.9(2)	30(2)	0.64(3)	$23/2^-$(b)	$\rightarrow$	$21/2^-$(b)	$M1/E2$
330.9(2)	5.8(5)		$9/2^+$(e)	$\rightarrow$	$9/2^+$(c)	$M1/E2$
339.6(2)	54(3)		$15/2^+$(d)	$\rightarrow$	$13/2^+$(c)	$M1/E2$
373.2(2)	<2.0		$13/2^+$(e)	$\rightarrow$	$11/2^+$(d)	$M1/E2$
401.4(2)	<2.0		$11/2^+$(d)	$\rightarrow$	$9/2^+$(e)	$M1/E2$
401.9(2)	15(1)	0.60(4)	$21/2^-$(b)	$\rightarrow$	$19/2^+$(d)	$E1$
438.8(2)	10.1(6)	0.66(5)	$23/2^-$(b)	$\rightarrow$	$21/2^+$(e)	$E1$
448.9(2)	2.6(2)		$15/2^+$(d)	$\rightarrow$	$11/2^+$(d)	$E2$
472.8(2)	13(2)		$21/2^-$(b)	$\rightarrow$		
483.4(2)	10(1)			$\rightarrow$	$9/2^+$(e)	
506.0(2)	18(1)		$17/2^+$(c)	$\rightarrow$	$15/2^+$(d)	$M1/E2$
506.0(2)	2.7(3)					
507.5(2)	27(2)	0.59(3)	$25/2^-$(a)	$\rightarrow$	$23/2^-$(b)	$M1/E2$
523.3(2)	5.0(5)			$\rightarrow$	$25/2^-$(a)	
547.0(2)	11(1)		$11/2^-$(b)	$\rightarrow$	$9/2^+$(c)	$E1$
560.9(2)	5.3(4)			$\rightarrow$	$17/2^+$(c)	
573.2(2)	3.0(3)		(e)	$\rightarrow$	$21/2^+$(e)	
620.2(2)	<2.0		$9/2^+$(e)	$\rightarrow$	$7/2^+$(d)	$M1/E2$
629.8(3)	2.9(2)					
631.5(2)	2.8(2)		(b)	$\rightarrow$	$35/2^-$(b)	
637.8(2)	8.2(6)					
646.9(2)	9.6(9)					
654.7(2)	3.0(3)		(e)		(e)	
664.5(4)	<2.0					
669.0(2)	2.4(2)					
688.4(2)	5.4(4)					
705.2(2)	11.3(8)	1.09(12)	$33/2^-$(a)	$\rightarrow$	$29/2^-$(a)	$E2$
721.1(2)	6.5(5)		$15/2^-$(b)	$\rightarrow$	$13/2^+$(c)	$E1$
741.4(2)	6.5(5)		$19/2^-$(b)	$\rightarrow$	$17/2^+$(c)	$E1$
755.6(2)	3.9(4)					
759.4(2)	7.8(6)		$31/2^-$(b)	$\rightarrow$	$27/2^-$(b)	$E2$
768.5(3)	11.3(5)		$7/2^+$(d)	$\rightarrow$	$5/2^+$(c)	$M1/E2$
771.5(2)	7.0(5)			$\rightarrow$	$17/2^+$(e)	
775.2(2)	5.5(5)		$13/2^+$(e)	$\rightarrow$	$9/2^+$(e)	$E2$
781.1(3)	3.6(8)			$\rightarrow$	$21/2^+$(e)	
783.8(3)	<2.0					
805.8(2)	15(1)			$\rightarrow$	$17/2^+$(c)	
837.7(2)	4.3(5)			$\rightarrow$	$19/2^+$(d)	

TABLE I. (*Continued*).

E_γ (keV)	I_γ (%)	DCO ratio	I_i^π	→	I_f^π	Multipolarity
841.7(2)	82(5)		$13/2^+$(c)	→	$9/2^+$(c)	$E2$
842.4(2)	4.2(6)		$19/2^+$(d)	→	$17/2^+$(e)	$M1/E2$
845.7(2)	16(1)		$17/2^+$(c)	→	$13/2^+$(c)	$E2$
854.2(3)	0.9(1)		(a)		(a)	
865.7(2)	4.2(4)	1.06(14) [b]	$19/2^-$(b)	→	$15/2^-$(b)	$E2$
866.6(2)	4.4(5)	1.06(14) [b]	$41/2^-$(a)	→	$37/2^-$(a)	$E2$
891.4(2)	6.3(6)					
947.4(5)	<2.0			→	$17/2^+$(e)	
1007.9(2)	4.1(4)					
1016.0(4)	4.3(4)		$15/2^-$(b)	→	$11/2^-$(b)	$E2$
1021.8(2)	4.7(5)		$11/2^+$(d)	→	$7/2^+$(d)	$E2$
1058.2(2)	$\equiv 100$		$9/2^+$(c)	→	$5/2^+$(c)	$E2$
1066.7(2)	16(1)		$29/2^-$(a)	→	$25/2^-$(a)	$E2$
1067.4(3)	4.8(5)	1.04(11)		→	$15/2^+$(d)	
1107.7(2)	12.4(8)		$27/2^-$(b)	→	$23/2^-$(b)	$E2$
1111.0(4)	3.4(3)		(a)	→	$15/2^-$(b)	
1126.0(2)	18(1)	0.97(12)	$21/2^+$(e)	→	$17/2^+$(e)	$E2$
1138.1(2)	15(1)	1.08(10)	$19/2^+$(d)	→	$15/2^+$(d)	$E2$
1161.2(2)	7.3(5)	0.99(9)	$37/2^-$(a)	→	$33/2^-$(a)	$E2$
1243.7(2)	3.4(3)		$21/2^-$(b)	→	$17/2^+$(e)	$M2$
1301.5(4)	4.3(3)		$35/2^-$(b)	→	$31/2^-$(b)	$E2$
1389.1(2)	12.6(9)		$9/2^+$(e)	→	$5/2^+$(c)	$E2$
1456.1(4)	<2.0		(a)	→	$41/2^-$(a)	

[a]Transition not observed directly in this experiment, but rather inferred from coincidence relationships. See text for details.

[b]DCO ratio includes unresolved contributions from both the 865.7- and 866.6-keV transitions.

determined to be in coincidence with the 705-keV $33/2^- \rightarrow 29/2^-$ transition. This implies that the level fed by the 1126-keV transition of band 1 has $I \geqslant 37/2\ \hbar$, if at least two units of spin are removed by the unobserved linking transitions. Similarly, a lower limit for the spins of band 2 was established by observing that transitions above and including the 371-keV transition are in coincidence with the 506- and 296-keV $17/2^+ \rightarrow 15/2^+$ transitions. The available experimental evidence does not allow firm parities to be assigned to these two bands. However, it was observed that band 1 predominantly feeds into sequences a and b (i.e., negative-parity levels), and the majority of the intensity of band 2 feeds into levels which have been assigned positive parity. Thus bands 1 and 2 are tentatively assigned negative and positive parity, respectively. The lower limits for the spins of the bands as estimated above are shown in Fig. 1. Note that since these spin assignments are lower limits the spin sequences shown in Fig. 1 cannot be used to assign a particular signature quantum number to the bands.

It should be noted that the spins of both bands may be considerably higher than the lower limits given above. In ^{109,111}Sb, the decay of the collective structures to the lower spin states has been found to be considerably fragmented [18,19,23]. It is therefore possible that there are much more than two units of spin between the band and the low-spin states as mentioned above. Also, given the low statistics in the present experiment, weak branches to states of very high spin have likely gone unobserved. This would tend to produce an unrealistically low spin estimate. Note also that the relatively uncomplicated linking of the positive-parity strongly coupled band in ^{109}Sb presented in both Refs. [18,19] is known to be incorrect; that band has significantly higher spins, is 2 MeV higher in excitation energy, and has a more fragmented decay than was previously published [24].

Two transitions which are shown in Fig. 1 were not directly observed in this experiment. These are the 47-keV transition which links the $21/2^-$ state in sequence b to a level with unassigned spin in sequence a, and the 77-keV transition linking the $15/2^+$ level of sequence d and the $13/2^+$ level of sequence e. The transitions were not observed since they have rather low intensity. These transitions are also somewhat absorbed by the Microball and highly converted due to their low energies. Their presence and position in the level scheme has been established through coincidence relationships.

IV. DISCUSSION

A. Low-spin shell-model states in ^{107}Sb

At low spins the level scheme of ^{107}Sb reveals no rotational structure; instead a collection of levels arising from single- and multiple-particle excitations is observed. Some of these levels result from the occupation of shell-model states

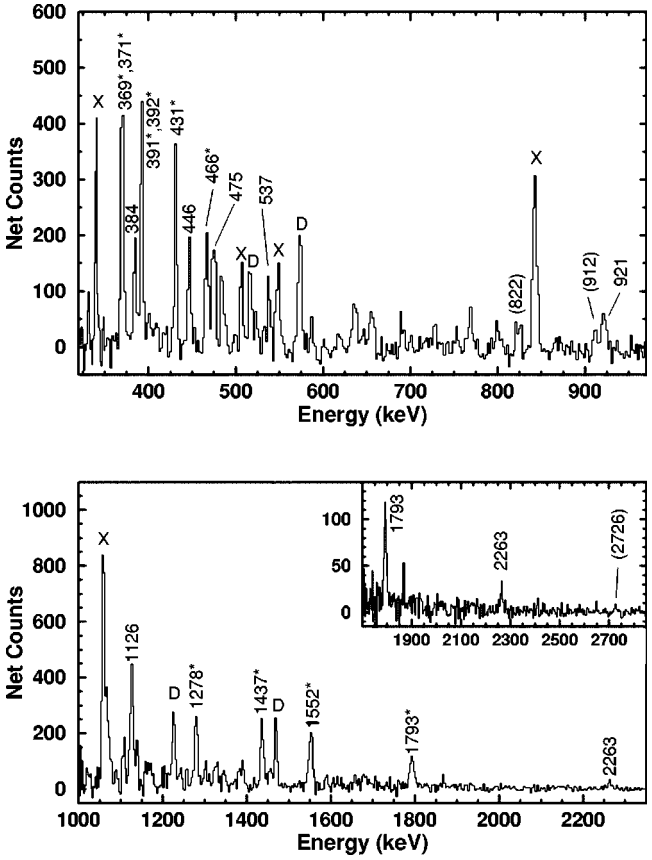

FIG. 2. Top: A spectrum showing the coupled band (band 2) identified in ^{107}Sb. The spectrum was generated by summing all combinations of double γ-ray energy gates on those transitions marked with an asterisk. Bottom: A spectrum showing the decoupled band (band 1) identified in ^{107}Sb. The spectrum was generated by summing single γ-ray energy gates on those transitions marked with an asterisk. The inset shows the high-energy portion of the same spectrum. In the top and bottom spectra, peaks marked with an X are known low-spin transitions in ^{107}Sb; those marked with a D are transitions involved in the partial decay-out of the band as shown in Fig. 1.

by the valence proton. The $I^{\pi}=5/2^{+}$ ground state, the $7/2^{+}$ excited state at 769 keV, and the $11/2^{-}$ state at 1605 keV result from the occupation of the $\pi d_{5/2}$, $\pi g_{7/2}$, and $\pi h_{11/2}$ orbitals, respectively. Each of these levels has a sequence of one or more $E2$ transitions feeding into it; these sequences can be naively interpreted as the coupling of the valence proton to the $0^{+}-2^{+}-4^{+}$ states of the underlying ^{106}Sn core. More than likely the states comprising the positive-parity sequences c, d, and e represent members of the multiplets which result from this coupling. Also, the positive-parity states probably have very mixed wavefunctions due to the near degeneracy of the $\pi d_{5/2}$ and $\pi g_{7/2}$ orbitals.

At higher excitation energies, spherical states can be generated by coupling the valence proton occupying a positive-parity orbital to a negative-parity excitation of the ^{106}Sn core. These core states are typically composed of a broken pair of neutrons, where one neutron occupies a $\nu h_{11/2}$ orbital, and the other occupies a $\nu d_{5/2}$ or $\nu g_{7/2}$ orbital. Such states having $I^{\pi}=19/2^{-}$ have been observed in several of the heavier odd-mass Sb isotopes, and found to be isomeric [23,25–27]. In the case of ^{107}Sb similar states are observed, for example the $I^{\pi}=19/2^{-}$ to $23/2^{-}$ states of sequence b. The state having $I^{\pi}=21/2^{-}$ may be isomeric; however, since the intensities which feed and depopulate this level are balanced, the half-life of this state must be short compared to the time of flight of the recoiling residual nucleus out of the target chamber. Thus the half-life of this state must be less than ≈ 10 ns.

TABLE II. Properties of γ transitions in ^{107}Sb belonging to collective bands 1 and 2. Tentative transitions have their energies reported in parentheses. Intensities have been normalized to the 1058.2-keV low-spin transition, as in Table I. The reported spins are lower limits, and along with the assigned multipolarities, should be considered tentative. See the text for details.

E_{γ} (keV)	I_{γ} (%)	I_i^{π}	$\rightarrow$	I_f^{π}	Multipolarity	Band
368.5(4)	6.0(5) [a]	21/2	$\rightarrow$	19/2	$M1/E2$	2
370.5(3)	6.0(5) [a]	23/2	$\rightarrow$	21/2	$M1/E2$	2
384.4(5)	1.8(4)	33/2	$\rightarrow$	31/2	$M1/E2$	2
391.2(2)	8.0(7) [b]	25/2	$\rightarrow$	23/2	$M1/E2$	2
392.3(3)	8.0(7) [b]	19/2	$\rightarrow$	17/2	$M1/E2$	2
430.8(3)	4.5(3)	27/2	$\rightarrow$	25/2	$M1/E2$	2
446.0(4)	2.2(4)	31/2	$\rightarrow$	29/2	$M1/E2$	2
466.4(5)	3.3(4)	29/2	$\rightarrow$	27/2	$M1/E2$	2
474.7(4)	2.0(5)	33/2	$\rightarrow$	31/2	$M1/E2$	2
516.2(4)	<1.0	21/2	$\rightarrow$			2
537.1(5)	1.8(5)	31/2	$\rightarrow$	29/2	$M1/E2$	2
572.0(5)	<1.0		$\rightarrow$			1
573.1(3)	<1.0		$\rightarrow$			2
(822)	<1.0	27/2	$\rightarrow$	23/2	$E2$	2
(912)	<1.0	31/2	$\rightarrow$	27/2	$E2$	2
920.5(6)	2.3(5)	33/2	$\rightarrow$	29/2	$E2$	2
1126.3(3)	2.3(5)	41/2	$\rightarrow$	37/2	$E2$	1
1225.8(4)	1.9(2)	37/2	$\rightarrow$			1
1278.4(3)	3.0(4)	45/2	$\rightarrow$	41/2	$E2$	1
1436.5(4)	3.5(4)	49/2	$\rightarrow$	45/2	$E2$	1
1469.4(4)	<1.0	37/2	$\rightarrow$			1
1552.1(4)	2.9(4)	53/2	$\rightarrow$	49/2	$E2$	1
1793.4(8)	1.0(3)	57/2	$\rightarrow$	53/2	$E2$	1
2263(1)	<1.0	61/2	$\rightarrow$	57/2	$E2$	1
(2726)	<1.0	65/2	$\rightarrow$	61/2	$E2$	1

[a]Reported intensity is the sum of the self-coincident 369- and 371-keV transitions.

[b]Reported intensity is the sum of the self-coincident 391- and 392-keV transitions.

B. The $\Delta I=2$ band 1

Even though the exact spins and parities of band 1 are unknown, it is still possible to understand its structure through comparison to both calculations and systematics. Decoupled rotational bands are now a well-established feature of nuclei near the $Z=50$ spherical shell gap (see Ref. [28], and references therein), having been observed in isotopes of $_{50}$Sn [2,29–32], $_{51}$Sb [1,5–7,18,23,33–35], and $_{52}$Te [20–22,36]. In the case of the heavier odd-mass

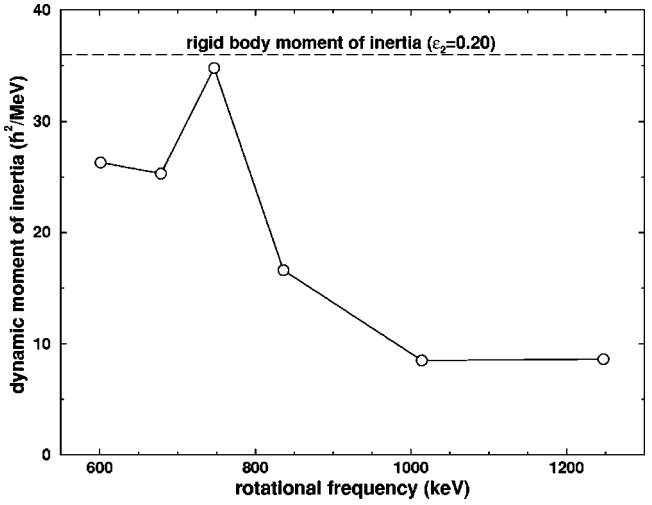

FIG. 3. The dynamic moment of inertia for band 1 in ^{107}Sb. The dashed line shows the moment of inertia for a rigid body having mass $A=107$ and deformation $\varepsilon_2=0.20$.

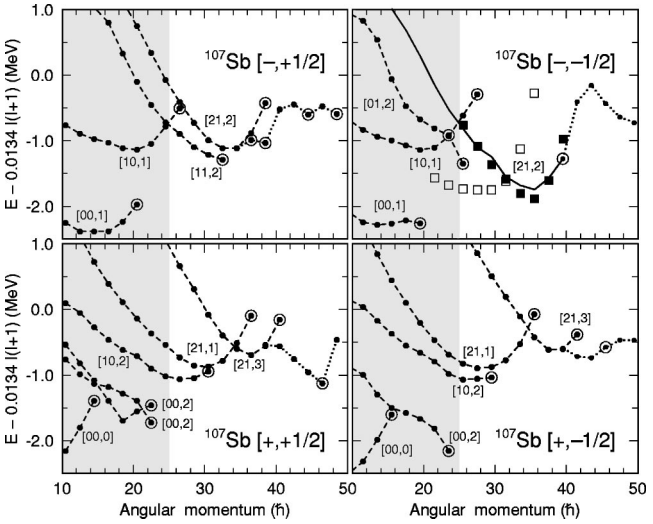

FIG. 4. Four plots showing the energies (minus a rigid-rotor reference) vs spin for the configurations calculated using the CNS approach. Each panel shows one of the four possible parity-signature combinations, as indicated. The configurations are labeled according to the convention described in the text. The shaded areas of the plots indicate the low-spin region where pairing may be significant, and therefore the calculations less reliable. The circled data points indicate the terminating states of the configurations. In the upper right-hand panel, the suggested experimental values for the decoupled band 1 are shown as filled squares. A set of experimental values based on an alternative spin assignment is shown as open squares.

$^{115-119}$Sb isotopes, the valence proton occupying a low-K orbital couples to the $2p$-$2h$ core excitation, resulting in as many as three rotational bands. The three bands result from the occupation of the $\pi h_{11/2}$ and mixed $\pi(d_{5/2}g_{7/2})$ orbitals by the valence proton. An illustrative example of this can be found in ^{117}Sb [6]. In the lighter isotopes, these three configurations and other proton excitations are frequently found coupled to neutron excitations as well. However, invariably the most intensely populated decoupled rotational band in the odd-mass $^{109-119}$Sb isotopes is based on the $\pi h_{11/2}$ valence proton coupled to the proton $2p$-$2h$ core excitation. Since the decoupled structure (band 1) observed in ^{107}Sb is tentatively assigned negative parity, the above arguments allow a tentative proton configuration assignment of $\pi h_{11/2} \otimes \pi(2p2h)$ to this structure.

As mentioned in the Introduction, a common feature of decoupled rotational bands in this mass region is band termination. Experimentally the gradual loss of collectivity synonymous with band termination in this mass region is manifest by an increase in the spacing of successive in-band transition energies, and hence a decrease in the dynamic moment of inertia ($\mathcal{J}^{(2)}$). Typically the $\mathcal{J}^{(2)}$ decreases to values well below that calculated for a rigid rotor having only modest deformation. In Fig. 3 the $\mathcal{J}^{(2)}$ of band 1 in ^{107}Sb is shown, along with the expected value of the moment of inertia for a rigid rotating body having a deformation of $\varepsilon_2=0.20$. The $\mathcal{J}^{(2)}$ of the band is seen to drop rather sharply as the rotational frequency increases; at the top of the band, the $\mathcal{J}^{(2)}$ is roughly one-fourth the rigid-body value. Both of these observations are consistent with smooth band termination taking place in this structure.

A more quantitative understanding of band 1 in ^{107}Sb is provided by calculations based on the configuration-dependent cranked Nilsson-Strutinsky (CNS) approach with the Nilsson potential. In this approach the nuclear energy is modeled as a rotating liquid drop with shell corrections based on level densities, and calculated for specific configurations of valence nucleons outside the ^{100}Sn core (including possible excitations from the $\pi g_{9/2}$ orbitals). The energy of each configuration at each spin is minimized in deformation space (ε_2, ε_4, γ) which allows the development of collectivity to be traced within specific configurations as a function of spin. Pairing is not included in this model, and thus the results can be considered reliable only at spins where pairing has become unimportant, roughly $I \geqslant 25\hbar$. A more detailed description of the CNS approach as it applies to nuclei near $Z=50$ can be found in Ref. [28], and references therein.

The results of the CNS calculations are shown in Figs. 4 and 5. They are displayed as energy minus a rigid-rotor ref-

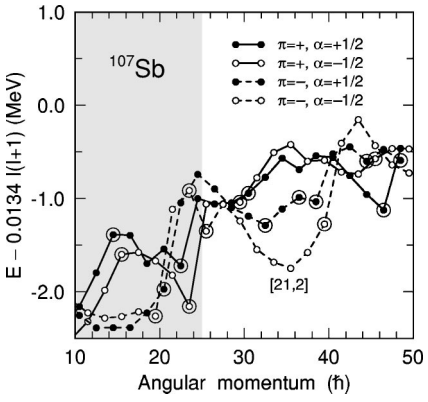

FIG. 5. Similar to Fig. 4, except that only the yrast states of each parity-signature combination are shown, regardless of configuration.

erence ($E-E_{\mathrm{RLD}}$) versus spin. Figure 4 shows the configurations forming the yrast line, separated according to the four combinations of parity and signature. Figure 5 shows only the yrast lines for each signature and parity combination. In both figures, the configurations are labeled according to the number of high-j orbitals involved in the configuration. The notation $[p_1p_2,n]$ denotes a configuration in which there are p_1 holes in the $\pi g_{9/2}$ orbitals, and p_2 (n) protons (neutrons) occupying the $h_{11/2}$ orbitals. Any remaining valence particles occupy the $g_{7/2}d_{5/2}$ orbitals.

Figure 4 reveals a large number of high-spin collective structures in ^{107}Sb. Many of these can be eliminated as candidate interpretations of band 1 based on simple arguments. The configurations with one hole in the $\pi g_{9/2}$ orbital ($[1n,m]$ in the shorthand notation) can be excluded since these configurations give rise to two signature partner bands having small signature splitting. In addition, these configurations terminate at spins below the maximum spin of band 1. The $[0n,m]$ configurations can also be eliminated since they possess small collectivity, and also terminate at spins lower than the highest observed spins of band 1. Thus the $[2n,m]$ configurations are the only reasonable interpretations for band 1.

Figure 5 shows that one $[2n,m]$ configuration in particular, the [21,2], is considerably more yrast than the others in the spin range of interest. This configuration has an expanded proton configuration of $\pi h_{11/2}\otimes[\pi(g_{9/2})^{-2}\otimes\pi(g_{7/2}d_{5/2})^2]$, and a $\nu(g_{7/2}d_{5/2})^4\otimes\nu(h_{11/2})^2$ configuration for the six valence neutrons. This matches the configuration tentatively assigned to this band in previous paragraphs based on the systematics of odd-mass $_{51}$Sb nuclei. It is also worth noting that there is an irregularity present in the $E-E_{\mathrm{RLD}}$ curve for this band (best seen in the upper right-hand panel of Fig. 4), which matches an irregularity observed in the $\mathcal{J}^{(2)}$ of band 1 (see Fig. 3). This irregularity is attributed to the crossing of $\pi(g_{7/2}d_{5/2})$ orbitals [28].

Comparing the shapes of the theoretical and experimental $E-E_{\mathrm{RLD}}$ curves, and in particular the minima of the curves, the best agreement is found with a spin assignment of $I_{\mathrm{min}}=51/2$ for the bottom state of the band (i.e., the level fed by the 1126-keV transition). The agreement can be seen in the upper-right panel of Fig. 4, where the experimental data have been overlaid as filled squares onto the calculations. An alternative spin assignment with $I_{\mathrm{min}}=43/2$ is shown for comparison in the figure using open square symbols. The alternative assignment does not match any of the theoretical curves. In addition, the uppermost states of the band become high in energy very quickly. If this alternative spin assignment is correct, these states would be far from yrast and should not be observed in the experiment. Thus the comparison between theory and experiment suggests that the spin of the bottom state of the band is $I_{\mathrm{min}}=51/2$. This assignment is consistent with the experimentally determined lower limit. Given this assignment, the calculations suggest that the uppermost (tentative) state of band 1 is in fact the terminating state of the band.

C. The $\Delta I=1$ band 2

In order to understand the structure of the sequence of $M1$ transitions labeled band 2 in Fig. 1 we first turn to systematics. Band 2 is reminiscent of a pair of strongly coupled bands, similar to those known in all the heavier odd-mass $^{109-123}$Sb nuclei [5–7,18,19,23,37,38]. Two such structures having opposite parities are known in those isotopes from mass $A=109$ to 119, with the exception of ^{113}Sb [37]. All of these structures have an underlying proton two-particle one-hole $\pi(g_{9/2})^{-1}\otimes\pi(g_{7/2}d_{5/2})^2$ configuration which is responsible for the deformation. The negative-parity bands couple this proton configuration to either the $I^{\pi}=5^-$ or 7^- two-neutron state of the underlying $_{50}$Sn core. These configurations have a high K value of 4.5 $\hbar$, which explains the lack of signature splitting in the bands and the large $B(M1)/B(E2)$ ratios.

The above described systematics allow some statements concerning the structure of band 2 to be made. This structure is apparently composed of two strongly coupled signature partners. Even though the transition energies are somewhat erratic, the splitting between the two signatures is very small over the length of the band. Since crossover $E2$ transitions were either not observed or have low intensity, the $B(M1)/B(E2)$ ratios of reduced transition probabilities for the levels of the band are rather large. These are indications that a high-K orbital is involved in the structure of this band. Thus we conclude that band 2 in ^{107}Sb involves the same $2p1h$ proton configuration as similar bands in the heavier odd-mass Sb isotopes.

From the experimental data it is not possible to determine whether the band is based on a positive- or negative-parity configuration. The CNS calculations indicate two strongly coupled structures, [10,1] (negative parity) and [10,2] (positive parity), based on one proton hole in the $\pi g_{9/2}$ orbital, which are reasonably low in energy at spin $I=10-25$ $\hbar$ (see Fig. 4). It should be pointed out that the band is observed to feed only into positive-parity states. Also worth noting is that the band branches out at the top, similar to what has been seen in the positive-parity strongly coupled band in ^{109}Sb [18].

In the recent literature, structures manifest as sequences of $M1$ transitions have been interpreted as ''shears bands'' using the tilted axis cranking (TAC) model [39]. The TAC model predicts regularly spaced sequences of $M1$ transitions having $B(M1)$ strengths that decrease with increasing spin, large $B(M1)/B(E2)$ ratios, and small deformations. In particular, this model has been successfully applied to nuclei near closed shells, for example ^{105,106,108}Sn [40–42] and ^{108}Sb [43]. Band 2 in ^{107}Sb is a good candidate for a shears band since it is expected to have low deformation [23], and is known to have large $B(M1)/B(E2)$ ratios. However, the lack of both firm spin assignments and lifetime measurements do not allow for a meaningful comparison to the predictions of the TAC model.

V. CONCLUSIONS

In conclusion, the neutron-deficient nucleus ^{107}Sb has been studied to high spin for the first time with a third-generation detector array, employing Gammasphere and the Microball. A large number of near-spherical states has been identified and interpreted as resulting from the coupling of

the valence proton to various states of the ^{106}Sn core. Two rotational structures have also been uncovered. One is a decoupled band, and has been assigned the full configuration $\pi h_{11/2}\otimes[\pi(g_{9/2})^{-2}\otimes\pi(g_{7/2}d_{5/2})^2]\otimes\nu(g_{7/2}d_{5/2})^4\otimes\nu(h_{11/2})^2$. Calculations using the cranked Nilsson-Strutinsky framework are consistent with the experimental observables and have been used to infer that this structure terminates at a spin of 79/2 $\hbar$. The second rotational structure is a weakly populated sequence of $M1$ transitions, which is interpreted as a strongly coupled band based on a high-K $\pi(g_{9/2})^{-1}\otimes\pi(g_{7/2}d_{5/2})^2$ proton configuration. The possibility of a tilted axis cranking interpretation for this structure was also discussed.

ACKNOWLEDGMENTS

This project has been funded in part by the U.S. National Science Foundation, the U.S. Department of Energy, the U.S. National Research Council under the Collaboration in Basic Science and Engineering Program, the U.K. Engineering and Physical Sciences Research Council, and the Swedish Natural Science Research Council.

[1] V. P. Janzen, H. R. Andrews, B. Haas, D. C. Radford, D. Ward, A. Omar, D. Prévost, M. Sawacki, P. Unrau, J. C. Waddington, T. E. Drake, A. Galindo-Uribarri, and R. Wyss, Phys. Rev. Lett. **70**, 1065 (1993).

[2] J. Bron, W. H. A. Hesselink, A. van Poelgeest, J. J. A. Zalmstra, M. J. Uitzinger, H. Verheul, K. Heyde, M. Waroquier, H. Vincx, and P. van Isacker, Nucl. Phys. **A318**, 335 (1979).

[3] A. K. Gaigalas, R. E. Shroy, G. Schatz, and D. B. Fossan, Phys. Rev. Lett. **35**, 555 (1975).

[4] R. E. Shroy, A. K. Gaigalas, G. Schatz, and D. B. Fossan, Phys. Rev. C **19**, 1324 (1979).

[5] R. S. Chakrawarthy and R. G. Pillay, Phys. Rev. C **54**, 2319 (1996).

[6] D. R. LaFosse, D. B. Fossan, J. R. Hughes, Y. Liang, P. Vaska, M. P. Waring, and J.-y. Zhang, Phys. Rev. Lett. **69**, 1332 (1992).

[7] D. R. LaFosse, D. B. Fossan, J. R. Hughes, Y. Liang, H. Schnare, P. Vaska, M. P. Waring, and J.-y. Zhang, Phys. Rev. C **56**, 760 (1997).

[8] Gammasphere Proposal, No. LBNL-PUB-5202; I. Y. Lee, Nucl. Phys. **A520**, 361 (1990).

[9] P. J. Nolan, F. A. Beck, and D. B. Fossan, Annu. Rev. Nucl. Part. Sci. **44**, 561 (1994).

[10] I. Ragnarsson, V. P. Janzen, D. B. Fossan, N. C. Schmeing, and R. Wadsworth, Phys. Rev. Lett. **74**, 3935 (1995).

[11] A. V. Afanasjev and I. Ragnarsson, Nucl. Phys. **A591**, 387 (1995).

[12] M. Devlin, L. G. Sobotka, D. G. Sarantites, and D. R. LaFosse, Nucl. Instrum. Methods Phys. Res. A **383**, 506 (1996).

[13] D. G. Sarantites, P. F. Hua, M. Devlin, L. G. Sobotka, J. Elson, J. T. Hood, D. R. LaFosse, J. E. Sarantites, and M. R. Maier, Nucl. Instrum. Methods Phys. Res. A **381**, 418 (1996).

[14] A. J. Boston, E. S. Paul, C. J. Chiara, M. Devlin, D. B. Fossan, S. J. Freeman, D. R. LaFosse, G. J. Lane, M. Leddy, I. Y. Lee, A. O. Macchiavelli, P. J. Nolan, D. G. Sarantites, J. M. Sears, A. T. Semple, J. F. Smith, and K. Starosta, Phys. Rev. C **61**, 064316 (2000).

[15] K. S. Krane, R. M. Steffen, and R. M. Wheeler, Nucl. Data Tables **11**, 351 (1973).

[16] D. C. Radford, Nucl. Instrum. Methods Phys. Res. A **361**, 297 (1995).

[17] D. Seweryniak, J. Cederkäll, B. Cederwall, J. Blomqvist, C. Fahlander, A. Johnson, L-O. Norlin, J. Nyberg, A. Atac, A. Kerek, J. Kownacki, R. Wyss, E. Adamides, H. Grawe, E. Ideguchi, R. Julin, S. Juutinen, W. Karczmarczyk, S. Mitarai, M. Piiparinen, R. Schubart, G. Sletten, S. Törmänen, and A. Virtanen, Phys. Lett. B **321**, 323 (1994).

[18] H. Schnare, D. R. LaFosse, D. B. Fossan, J. R. Hughes, P. Vaska, K. Hauschild, I. M. Hibbert, R. Wadsworth, V. P. Janzen, D. C. Radford, S. M. Mullins, C. W. Beausang, E. S. Paul, J. DeGraaf, I. Y. Lee, A. O. Macchiavelli, A. V. Afanasjev, and I. Ragnarsson, Phys. Rev. C **54**, 1598 (1996).

[19] T. Ishii, A. Makishima, M. Shibata, M. Ogawa, and M. Ishii, Phys. Rev. C **49**, 2982 (1994).

[20] E. S. Paul, H. R. Andrews, T. E. Drake, J. DeGraaf, V. P. Janzen, S. Pilotte, D. C. Radford, and D. Ward, Phys. Rev. C **50**, R534 (1994).

[21] A. J. Boston, E. S. Paul, C. J. Chiara, M. Devlin, D. B. Fossan, D. R. LaFosse, G. J. Lane, I. Y. Lee, A. O. Macchiavelli, P. J. Nolan, D. G. Sarantites, J. M. Sears, A. T. Semple, J. F. Smith, and K. Starosta (to be published).

[22] E. S. Paul, C. W. Beausang, S. A. Forbes, S. J. Gale, A. N. James, P. M. Jones, M. J. Joyce, H. R. Andrews, V. P. Janzen, D. C. Radford, D. Ward, R. M. Clark, K. Hauschild, I. M. Hibbert, R. Wadsworth, R. A. Cunningham, J. Simpson, T. Davinson, R. D. Page, P. J. Sellin, P. J. Woods, D. B. Fossan, D. R. LaFosse, H. Schnare, M. P. Waring, A. Gizon, J. Gizon, T. E. Drake, J. DeGraaf, and S. Pilotte, Phys. Rev. C **50**, 698 (1994).

[23] D. R. LaFosse, D. B. Fossan, J. R. Hughes, Y. Liang, H. Schnare, P. Vaska, M. P. Waring, J.-Y. Zhang, R. M. Clark, R. Wadsworth, S. A. Forbes, E. S. Paul, V. P. Janzen, A. Galindo-Uribarri, D. C. Radford, D. Ward, S. M. Mullins, D. Prevost, and G. Zwartz, Phys. Rev. C **50**, 1819 (1994).

[24] G. J. Lane *et al.* (unpublished).

[25] L. K. Kostov, W. Andrejtscheff, L. G. Kostova, A. Dewald, G. Böhm, K. O. Zell, P. von Brentano, H. Prade, J. Döring, and R. Schwengner, Z. Phys. A **337**, 407 (1990).

[26] S. R. Faber, L. E. Young, and F. M. Bernthal, Phys. Rev. C **19**, 720 (1979).

[27] J. Konijn, T. J. Ketel, and H. Verheul, Z. Phys. A **289**, 287 (1979).

[28] A. V. Afanasjev, D. B. Fossan, G. J. Lane, and I. Ragnarsson, Phys. Rep. **322**, 1 (1999).

[29] R. Wadsworth, H. R. Andrews, C. W. Beausang, R. M. Clark, J. DeGraaf, D. B. Fossan, A. Galindo-Uribarri, I. M. Hibbert, K. Hauschild, J. R. Hughes, V. P. Janzen, D. R. LaFosse, S. M. Mullins, E. S. Paul, L. Persson, S. Pilotte, D. C. Radford, H.

Schnare, P. Vaska, D. Ward, J. N. Wilson, and I. Ragnarsson, Phys. Rev. C **50**, 483 (1994).

[30] R. Wadsworth, H. R. Andrews, R. M. Clark, D. B. Fossan, A. Galindo-Uribarri, J. R. Hughes, V. P. Janzen, D. R. LaFosse, S. M. Mullins, E. S. Paul, D. C. Radford, H. Schnare, P. Vaska, D. Ward, J. N. Wilson, and R. Wyss, Nucl. Phys. **A559**, 461 (1993).

[31] D. R. LaFosse, D. B. Fossan, J. R. Hughes, Y. Liang, P. Vaska, M. P. Waring, J.-y. Zhang, R. M. Clark, R. Wadsworth, S. A. Forbes, and E. S. Paul, Phys. Rev. C **51**, R2876 (1995).

[32] J. M. Sears, S. E. Gundel, D. B. Fossan, D. R. LaFosse, P. Vaska, J. DeGraaf, T. E. Drake, V. P. Janzen, D. C. Radford, Ch. Droste, T. Morek, U. Garg, K. Lamkin, S. Naguleswaran, G. Smith, J. C. Walpe, R. Kaczarowski, A. V. Afanasjev, and I. Ragnarsson, Phys. Rev. C **58**, 1430 (1998).

[33] V. P. Janzen, D. R. LaFosse, H. Schnare, D. B. Fossan, A. Galindo-Uribarri, J. R. Hughes, S. M. Mullins, E. S. Paul, L. Persson, S. Pilotte, D. C. Radford, I. Ragnarsson, P. Vaska, J. C. Waddington, R. Wadsworth, D. Ward, J. Wilson, and R. Wyss, Phys. Rev. Lett. **72**, 1160 (1994).

[34] G. J. Lane, D. B. Fossan, I. Thorslund, P. Vaska, R. G. Allatt, E. S. Paul, L. Käubler, H. Schnare, I. M. Hibbert, N. O'Brien, R. Wadsworth, W. Andrejtscheff, J. DeGraaf, J. Simpson, I. Y. Lee, A. O. Macchiavelli, D. J. Blumenthal, C. N. Davids, C. J. Lister, D. Seweryniak, A. V. Afanasjev, and I. Ragnarsson, Phys. Rev. C **55**, R2127 (1997).

[35] G. J. Lane, D. B. Fossan, C. J. Chiara, H. Schnare, J. M. Sears, J. F. Smith, I. Thorslund, P. Vaska, E. S. Paul, A. N. Wilson, K. Hauschild, I. M. Hibbert, R. Wadsworth, A. V. Afanasjev, and I. Ragnarsson, Phys. Rev. C **58**, 127 (1998).

[36] I. Thorslund, D. R. LaFosse, H. Schnare, K. Hauschild, I. M. Hibbert, S. M. Mullins, E. S. Paul, I. Ragnarsson, J. M. Sears, P. Vaska, and R. Wadsworth, Phys. Rev. C **52**, R2839 (1995).

[37] C.-B. Moon, C. S. Lee, J. C. Kim, J. H. Ha, T. Komatsubara, T. Shizuma, K. Uchiyama, K. Matsuura, M. Murasaki, Y. Sasaki, H. Takahashi, Y. Tokita, and K. Furuno, Phys. Rev. C **58**, 1833 (1998).

[38] W. F. Piel, Jr., P. Chowdhury, U. Garg, M. A. Quader, P. M. Stwertka, S. Vajda, and D. B. Fossan, Phys. Rev. C **31**, 456 (1985).

[39] S. Frauendorf, Nucl. Phys. **A557**, 259c (1993).

[40] A. Gadea, G. de Angelis, C. Fahlander, M. De Poli, E. Farnea, Y. Li, D. R. Napoli, Q. Pan, P. Spolaore, D. Bazzacco, S. M. Lenzi, S. Lunardi, C. M. Petrache, F. Brandolini, P. Pavan, C. Rossi Alvarez, M. Sferrazza, P. G. Bizzeti, A. M. Bizzeti Sona, J. Nyberg, M. Lipoglavsek, J. Persson, J. Cederkäll, D. Seweryniak, A. Johnson, H. Grawe, F. Soramel, M. Ogawa, A. Makishima, R. Schubart, and S. Frauendorf, Phys. Rev. C **55**, R1 (1997).

[41] D. G. Jenkins, I. M. Hibbert, C. M. Parry, R. Wadsworth, D. B. Fossan, G. J. Lane, J. M. Sears, J. F. Smith, R. M. Clark, R. Krücken, I. Y. Lee, A. O. Macchiavelli, V. P. Janzen, J. Cameron, and S. Frauendorf, Phys. Lett. B **428**, 23 (1998).

[42] D. G. Jenkins, R. Wadsworth, J. A. Cameron, R. M. Clark, D. B. Fossan, I. M. Hibbert, V. P. Janzen, R. Krücken, G. J. Lane, I. Y. Lee, A. O. Macchiavelli, C. M. Parry, J. M. Sears, J. F. Smith, and S. Frauendorf, Phys. Rev. Lett. **83**, 500 (1999).

[43] D. G. Jenkins, R. Wadsworth, J. Cameron, R. M. Clark, D. B. Fossan, I. M. Hibbert, V. P. Janzen, R. Krücken, G. J. Lane, I. Y. Lee, A. O. Macchiavelli, C. M. Parry, J. M. Sears, J. F. Smith, and S. Frauendorf, Phys. Rev. C **58**, 2703 (1998).